

Spin dynamics of the potassium magnetometer in spin-exchange relaxation free regime*

Ji-Qing Fu(伏吉庆)¹, Peng-Cheng Du(杜鹏程)², Qing Zhou(周庆)², and Ru-Quan Wang(王如泉)^{1,†}

¹*Institute of Physics, Chinese Academy of Sciences, Beijing 100190, China*

²*School of Physical Science and Technology, Yunnan University, Kunming 650091, China*

(Received 19 October 2015; revised manuscript received 5 November 2015; published online 30 November 2015)

The laser-pumped potassium spin-exchange relaxation free (SERF) magnetometer is the most sensitive detector of magnetic field and has many important applications. We present the experimental results of our potassium SERF magnetometer. A pump-probe approach is used to identify the unique spin dynamics of the atomic ensemble in the SERF regime. A single channel sensitivity of $8 \text{ f}\cdot\text{THz}^{-1/2}$ is achieved with our SERF magnetometer.

Keywords: Larmor process, spin-exchange relaxation free magnetometer, atomic magnetometer

PACS: 03.65.Sq, 32.30.Dx, 32.50.+d, 33.57.+c

DOI: 10.1088/1674-1056/25/1/010302

1. Introduction

The light-pumped atomic magnetometer is one of the most important high sensitivity magnetometers,^[1–5] it has a sensitivity orders of magnitude better than the fluxgate magnetometer and magnetometers based on the Hall effect^[6] and the magnet GMR^[7] effect. Besides the advantage of sensitivity, the atomic magnetometer does not require cryogenic cooling as the superconducting quantum interference device (SQUID) magnetometer, and offers great potential for miniaturization.^[8]

In the last decade, the spin-exchange relaxation free (SERF) atomic magnetometer^[9,10] has significantly improved the sensitivity of the atomic magnetometers. With the reported sensitivity of $0.16 \text{ f}\cdot\text{THz}^{-1/2}$ ^[11] and the projected fundamental limits below $2 \text{ a}\cdot\text{THz}^{-1/2}$,^[12] the sensitivity of the SERF magnetometer rivals and even surpasses that of the best low temperature SQUID magnetometer.^[13] In recent years, significant progress has been witnessed in the development of the SERF magnetometer.^[14,16–20] As a result, the SERF magnetometer has found many important applications where ultra high sensitive magnetic field measurements are required. For example, the precision measurement of the electron electric dipole moments (EDM) can provide critical constraints of parameters for theories beyond the standard model,^[21] the investigation of the tiny magnetization field in ancient rocks is very important for the paleomagnetism research,^[11] and the geo-magnetic anomalies measurement is a powerful tool in mining and the anti-submarine warfare.^[22] Furthermore, the SERF magnetometer is well suited for biomagnetic measurements, there are already successful applications of the SERF magnetometer in magnetoencephalography (MEG)^[23] and magneto-cardiography (MCG).^[24]

In this paper, we present our experimental results of the potassium SERF magnetometer. We will first discuss the SERF mechanism, then we will describe the details of our experimental setup. Because it is very important to identify the SERF and non-SERF regimes, we will next present a pump-probe experiment for this purpose. Finally, we will show our magnetometer signal and the noise spectrum, which indicate a single channel sensitivity of $8 \text{ f}\cdot\text{THz}^{-1/2}$.

2. The SERF mechanism

The sensitivity of the atomic magnetometer is limited by the coherence time of the atomic ensemble, and one of the most important decoherence mechanisms is the spin-exchange collisions. The spin-exchange collisions are the collisions between the alkali atoms which conserve the total spin of the colliding atoms but flip the electron spin of each of the atoms. The spin-exchange collisions lead to random transfers between the two ground state hyperfine levels of the atoms, which have the opposite directions of Larmor precession. When the atoms precess in different directions and at different angular speeds with each other, the total spin of the atomic ensemble become smaller, which leads to the spin relaxation of the atomic ensemble.

Demonstrated by Happer *et al.*,^[25,26] the effects of the spin-exchange relaxation can be suppressed in the SERF regime, when the spin-exchange rate is much larger than the Larmor precession frequency. In the SERF regime, the atoms go through many spin-exchange collisions during one cycle of Larmor precession, being quickly switched between different ground states, each atom will go through the same average precession rate, so they remain synchronized in the precession process and do not suffer from the decoherence any more.

*Project supported by the National Natural Science Foundation of China (Grant No. 61227902).

†Corresponding author. E-mail: ruquanwang@aphy.iphy.ac.cn

© 2016 Chinese Physical Society and IOP Publishing Ltd

<http://iopscience.iop.org/cpb> <http://cpb.iphy.ac.cn>

3. The experimental setup and magnetometer signal

The experimental setup of the potassium SERF magnetometer is shown in Fig. 1. The potassium atoms are contained in a cubic glass cell, the size of the cell is 2.5 cm. The cell is filled with 450 torr of ^4He gas and 60 torr of N_2 gas. The ^4He gas works as the buffer gas, the buffer gas makes the atoms go through random walks in the glass cell and significantly reduces the wall collisions of the atoms. Since the wall collisions change the atomic spin, the use of the buffer gas can greatly reduce the decoherence rate of the atoms. The N_2 gas works as the quenching gas to absorb the energy of the states excited by the optical pumping light, so that they will not randomly emit photons which can destroy the polarization of the atomic ensemble; this is very important in an atomic ensemble with a very large optical depth because photons can be trapped in the ensemble and affect multiple atoms before they leave the ensemble. The cell is placed in an oven made by borazon and heated to 150 °C by resistive heating of a 22 kHz AC current. At this temperature, the density of the potassium gas is much higher than that at the room temperature, which leads to a much higher spin-exchange rate and ensures the working condition for the SERF magnetometer.

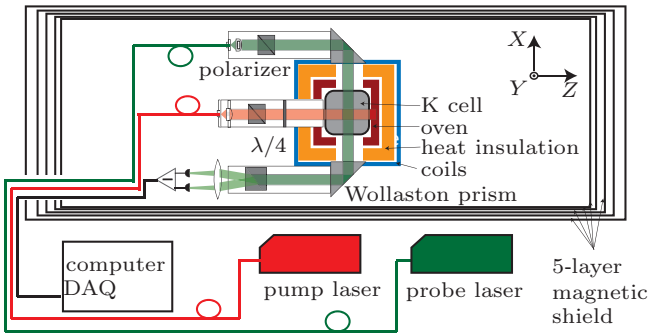


Fig. 1. Experimental implementation of the K magnetometer. Transverse polarization is detected using optical rotation.

We use a five-layer μ -metal magnetic shield with an expected shielding factor of 10^9 to isolate the system from the ambient magnetic field. The geometry of the shield is optimized with both theoretical calculations and finite element numerical simulations. The diameters of the inner and outer shields are 16 cm and 35 cm, the lengths of the inner and outer shields are 53 cm and 73 cm, respectively. A set of coils inside the shields allows the control of the magnetic field in the x , y , and z directions. The potassium atoms are optically pumped by a circularly polarized light tuned to the D1 line from a diode laser (Toptica DL100). A linearly polarized light from a diode laser (Toptica DLpro) 68 GHz red detuned from the D2 line is used to probe the polarization of the atoms. Both pump and probe lasers are Gaussian beams with diameter (full width at half maximum) of 4 mm.

The atoms are polarized by the optical pumping beam along the z direction, their transverse polarization P_x caused by the magnetic field along the y direction is measured from the optical rotation angle of the linear polarized probe beam propagating along the x direction.

From the Bloch equation,^[12,27–29] the optical rotation angle of the linearly polarized probe light is a dispersive function in the regime near zero magnetic field

$$\theta = \frac{\pi}{2} l n_k r_e c f P_x D(\nu), \quad (1)$$

where l is the length of the pump–probe beams cross region, n_k is the number density of the potassium atoms, $r_e = 2.8 \times 10^{-13}$ cm is the classical radius of the electron, c is the speed of light, f is the oscillator strength (0.324 for D1 and 0.652 for D2), P_x is the polarization projection in the direction of the probe light from the steady-state solution of the Bloch equation, and $D(\nu) = (\nu - \nu_0) / [(\Delta\nu/2)^2 + (\nu - \nu_0)^2]$ is the imaginary component of the Voigt profile with full width at half maximum $\Delta\nu$ of the optical transition of frequency ν_0 .

In the experiment, we slowly scan B_y from -7 nT to 7 nT, the polarization rotation angle of the probe light is shown in Fig. 2. For a pumping beam power of 1 mW and a probe beam power of 0.5 mW, the magnetometer output is a dispersive curve with a 1.7 nT line width and a 7 mrad/nT slope in the linear response regime.

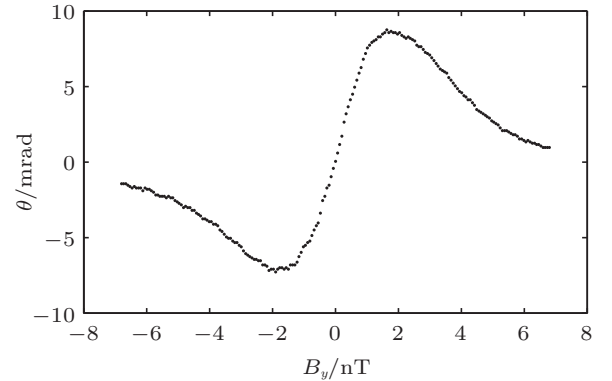


Fig. 2. Polarization rotation angle of the probe beam as a function of B_y , showing a dispersive line shape with a line width of 1.7 nT and a zero crossing slope of 7 mrad/nT.

4. Spin dynamic with pump–probe measurement

It is very important to clarify whether the magnetometer is running in the SERF regime or not in the experiment. Usually, people can find some evidence from the signal of the magnetometer such as those shown in Fig. 2, because in the SERF regime, suppression of the spin-exchange decoherence leads to a narrower linewidth. But the linewidth, which is determined by T_2 , is related to many other experimental conditions, which makes the experimental debugging process much

more complicated. Sometimes, it is hard to find which factor makes the greatest contribution to T_2 . For example, decoherence due to the wall collisions can dominate T_2 when the buffer gas pressure is inappropriate, the size of the cell is very small, or the coating of the cell does not work. The density of the atomic vapor can be different by orders of magnitude when the temperature of the glass cell changes for just tens of degrees, which will change both the spin-exchange decoherence rate and the spin-destruction decoherence rate by orders of magnitude. The impurities in the atomic gas can lead to significant broadening of the linewidth. Large ambient magnetic field noise can also cause a much broader magnetometer linewidth. So judging whether the atomic magnetometer is running in the SERF regime from the linewidth is not an ideal approach.

In this paper, we use a pump-probe approach to study the spin dynamics in the magnetometer. By observing the time-dependent damped precession signal, we can find direct evidence for whether the magnetometer works in the SERF regime or not. The time sequence of the experiment is shown in Fig. 3(a). We first apply a 50 ms pump beam to polarize the atom spins along the z direction, then a 9 nT magnetic field is turned on in the y direction, the atomic ensemble would go through free precession in this field. The linear polarized probe beam can measure the spin projection of the atomic ensemble in the x direction, just as done in the SERF magnetometer. The time-dependent solution to the Bloch equation is^[30]

$$P_x = P_0 e^{-t/\tau} \sin(\omega_y t + \phi), \quad (2)$$

where ω_y is the precession rate. In the non-SERF regime, $\omega_y = \omega_L$, where ω_L is the Larmor precession rate of the free atoms, while in the SERF regime, the spin precession rate is a factor of $3(2I+1)/[3+4I(I+1)]$ smaller than that in the non-SERF regime.^[12] For potassium, with nuclear spin $I = 3/2$, $\omega_y = (2/3)\omega_L$. The transverse relaxation rate $\tau = 1/T_2$ is dominated by the spin-exchange rate in the non-SERF regime and by the spin-destruction rate in the SERF regime.^[31,32]

The difference of the spin precession rate in the SERF and non-SERF regimes gives the best evidence of SERF regime in the experiment, because the precession rate is only related to the nuclear spin of the atoms which is precisely known, and the external magnetic field which can be easily measured. The experiment can also be done in the SERF and non-SERF regimes under the same external magnetic field by changing only the temperature of the vapor cell, the ratio of the precession rate is thus not related to the magnetic field, making the result even clearer.

In our experiment, we measure the spin precession rate at the temperatures of 85 °C (Fig. 3(b)) and 150 °C (Fig. 3(c)), and the time-dependent signal is fitted to Eq. (2) to obtain the precession rate and the decay time.

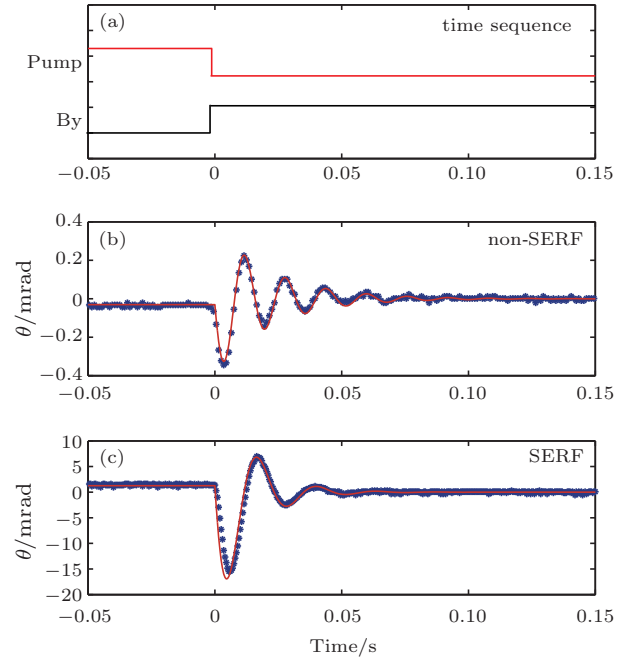


Fig. 3. The pump-probe signal. (a) Atomic spin is first polarized by a 50 ms pump laser pulse and then goes through free precession in a 9 nT bias field. The polarization rotation angles of the detection beam at vapor cell temperatures of (b) 85 °C and (c) 150 °C. The red lines are fitted lines with the Bloch equation. From the fit, the precession frequencies are 63 Hz and 42 Hz, and the relaxation rates are 54 s^{-1} and 77 s^{-1} in panels (b) and (c), respectively.

From the fit, in the presence of 9 nT magnetic field, the precession frequency is 63 Hz at 85 °C, which is in good agreement with the Larmor precess frequency of free atoms, but at 150 °C, the precession frequency is 42 Hz, which is clearly slower than the former and in good agreement with the prediction from the SERF theory (Eq. (2)). This is direct evidence for the magnetometer running in the SERF regime. The relaxation rate of the spin polarization does not have a significant difference from 85 °C to 150 °C, even when the spin-exchange rate is increased by 75 times. For $n_k \approx 1.8 \times 10^{13} \text{ cm}^{-3}$ at 150 °C, obtained from the saturated vapor pressure curve, the spin-exchange rate is about $R_{SE} = 15818 \text{ s}^{-1}$, which corresponds to a lifetime of 63 μs . From Fig. 3(c), we obtain a relaxation rate of 77 s^{-1} and a lifetime of $T_2 = 21 \text{ ms}$, which indicate that the spin-exchange relaxation effect is eliminated.

5. Sensitivity

In order to calibrate the sensitivity of the SERF magnetometer, a sinusoidal calibration field of $B_{\text{rms}} = 120 \text{ pT}$ at 20 Hz is applied, the sensitivity data are obtained by recording the output of the magnetometer for 100 s, performing a fast Fourier transform (FFT) without windowing, and calculating the r.m.s. amplitudes in 1 Hz bins,^[9] as shown in Fig. 4.

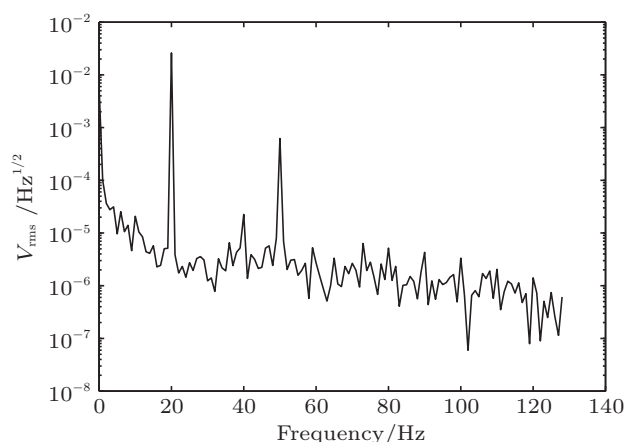


Fig. 4. Noise spectrum of the magnetometer signal with $B_y = 120$ pT applied at 20 Hz, giving a sensitivity of $8 \text{ f}\cdot\text{THz}^{-1/2}$.

Apart from several peaks from technical noise, the magnetic sensitivity is $8 \text{ f}\cdot\text{THz}^{-1/2}$ at 20 Hz. Further improvement of the sensitivity can be achieved by improving the performance of the magnetic shield and reducing the noise from the electronics and optical system.

6. Conclusion

In summary, we have successfully set up a potassium atomic SERF magnetometer and achieved a magnetometer sensitivity of $8 \text{ f}\cdot\text{THz}^{-1/2}$. A pump and probe experiment is conducted to measure the spin precession frequency and relaxation time, which clearly prove that our magnetometer is working in the SERF regime. The sensitivity of our magnetometer ranks among the best in the world, further research and application of the SERF magnetometer will be possible in the near future.

References

- [1] Kastler A 1950 *J. Phys. Radium* **11** 255
- [2] Dehmelt H 1957 *Phys. Rev.* **105** 1924
- [3] Bell W and Bloom A 1957 *Phys. Rev.* **107** 1559
- [4] Budker D, Gawlik W, Kimball D F, Rochester S M, Yashchuk V V and Weis A 2002 *Rev. Mod. Phys.* **74** 1153
- [5] Li S G, Xu Y F, Wang Z Y, Liu Y X and Lin Q 2009 *Chin. Phys. Lett.* **26** 067805
- [6] Edward R 2006 *Hall-effect Sensors: Theory and Applications* (New York: Elsevier)
- [7] Hirota E, Sakakima H and Inomata K 2002 *Giant Magneto-Resistance Devices* (Berlin: Springer) p. 23
- [8] Liew L, Knappe S, Moreland J, Robinson H, Hollberg L and Kitching J 2004 *Appl. Phys. Lett.* **84** 2694
- [9] Kominis I K, Kornack T W, Allred J C and Romalis M V 2003 *Nature* **422** 596
- [10] Budker D and Romalis M V 2007 *Nat. Phys.* **3** 227
- [11] Dang H B, Maloof A C and Romalis M V 2010 *Appl. Phys. Lett.* **97** 151110
- [12] Allred J C, Lyman R N, Kornack T W and Romalis M V 2002 *Phys. Rev. Lett.* **89** 130801
- [13] Clarke J and Braginski A I 2004 *The SQUID Handbook* (New York: Wiley-VCH, Weinheim)
- [14] Lee H J, Shim J H, Moon H S and Kim K 2014 *Opt. Express* **22** 17
- [15] Fang J C, Wan S G, Qin J, Zhang C and Quan W 2014 *J. Opt. Soc. Am. B* **31** 3
- [16] Wyllie R, Kauer M, Smetana G S, Wakai R T and Gwarker T 2012 *Phys. Med. Biol.* **57** 2619
- [17] Romalis M V 2010 *Phys. Rev. Lett.* **105** 243001
- [18] Yosuke I, Hiroyuki O, Keigo K and Tetsuo K 2012 *AIP Adv.* **2** 032127
- [19] Fang J C, Wang T, Zhang H, Li Y and Zou S 2014 *Rev. Sci. Instr.* **85** 123104
- [20] Griffith W C, Knappe S and Kitching J 2010 *Opt. Express* **18** 26
- [21] Kornack T W, Vasilakis G and Romalis M V 2008 *CPT and Lorentz Symmetry IV* pp. 206–213
- [22] Billings S, Shubitidze F, Pasion L, Beran L and Foley J 2010 *Requirements for Unexploded Ordnance Detection and Discrimination in the Marine Environment Using Magnetic and Electromagnetic Sensors* (Proceedings of OCEANS, IEEE-Sidney) p. 18
- [23] Xia H, Baranga A B, Hoffman D and Romalis M V 2006 *Appl. Phys. Lett.* **89** 211104
- [24] Bison G, Wynands R and Weis A 2003 *Appl. Phys. B* **76** 325
- [25] Happer W and Tang H 1973 *Phys. Rev. Lett.* **31** 273
- [26] Happer W and Tam A C 1977 *Phys. Rev. A* **16** 1877
- [27] Bloch F 1946 *Phys. Rev.* **70** 460
- [28] Appelt S, Ben-Amar B A, Erickson C J, Romalis M V, Young A R and Happer W 1998 *Phys. Rev. A* **58** 1412
- [29] Budker D and Kimball D F 2013 *Optical Magnetometry* (New York: Cambridge University Press)
- [30] Gusarov A, Levron D, Baranga A B, Paperno E and Shuker R 2011 *J. Appl. Phys.* **109** 07E507
- [31] Erickson C J, Levron D, Happer W, Kadlecsek S, Chann B, Anderson L W and Walker T G 2000 *Phys. Rev. Lett.* **85** 4237
- [32] Kadlecsek S, Anderson L W and Walker T G 1998 *Phys. Rev. Lett.* **80** 5512